

---

# Introduction

The Sun plays a vital role for virtually all lifeforms on earth, and its observation by humans is probably as old as mankind. Prehistoric cave drawings in Lascaux (France) indicate that people put the Sun and other celestial bodies into context with their daily life as early as 15.000 BC (Rappenglück, 2004a,b). The development of agriculture made it important to forecast the annual seed and harvest times, increasing the need for solar observation. Constructions like Stonehenge, the Pyramids of Gizeh and artifacts like the Nebra sky disk show that our ancestors had a precise knowledge of the yearly occurrence of the summer and winter solstice as well as the equinoxes in-between. Astronomy and mathematics were used by early civilizations to define a detailed calendar predicting phenomena such as the variation in the length of daylight over a solar year, the first and last visible risings of different planets over a period of decades and the prediction of solar and lunar eclipses. One of the oldest historical evidences of an astronomical incident is the solar eclipse recorded 2137 BC in China (Wang and Siscoe, 1980), and Aristarchus of Samos (310 BC - 230 BC), a supporter of the heliocentric system, estimated the distance between the Earth, the Moon and the Sun more than two thousand years ago (Heath, 1913).

In the following millennia, numerous scientists, e.g. Nicholas Copernicus, Galileo Galilei, Isaac Newton, William Herschel, Joseph von Fraunhofer, Lord Kelvin, Hermann von Helmholtz, Albert Einstein, Sir Arthur Eddington, Subrahmanyan Chandrasekhar and Hans Bethe, contributed to our modern picture of the Sun. Their work was aided by a steady improvement of scientific instruments and a fruitful exchange between the different branches of science. Famous examples of this interdisciplinary work include: a) Spectroscopic observation of sunlight, which led to the discovery of the hitherto unknown element helium. b) The long lasting controversy between geological and astrophysical measurements about the age of the Sun, which was not settled until the discovery of nuclear fusion (von Weizsäcker, 1938; Bethe, 1939). c) The discrepancy between the flux of solar neutrinos measured at earth and theoretical predictions, which finally led to the postulation of neutrino oscillations (Mikheyev and Smirnov, 1985). Besides evident facts such as its impact on the terrestrial weather and climate (Jungclaus et al., 2010), the Sun still influences our daily life in many ways. Modern communication via satellites, for example, is very prone to solar activity, and solar storms can cause power failures.

The Sun's stellar classification is G2V, accounting for its surface temperature of 5780 K and its location within the main sequence of the Hertzsprung-Russell-Diagram (Hertzsprung, 1909; Russell, 1914). At an age of  $4.86 \cdot 10^9$  years, it has completed about half of the main-sequence evolution. The Sun has a diameter of about  $1.4 \cdot 10^9$  m, a mass of  $2 \cdot 10^{30}$  kg and a luminosity of  $3.8 \cdot 10^{26}$  W (Unsöld and Baschek, 2002). On Earth, it appears as the brightest object in the sky ( $\text{mag} = -26.74$ ), even though its absolute magnitude is only +4.83. About 75% of its mass consists of hydrogen H, while the rest is mostly He. Less than 2% consist of heavier elements, including carbon (C), nitrogen (N), oxygen (O), neon (Ne), calcium (Ca), iron (Fe) and others. This composition is typical for a Population I star of the galactic disk; Population II stars from the halo of the Milky Way contain much less heavy elements. Out of the  $10^{23}$  estimated stars in the universe (van Dokkum and Conroy, 2010), the Sun is exceptional only in its proximity to Earth. This vicinity makes it a unique laboratory to test computer models and theoretical predictions, since it is the only star for which surface phenomena can be resolved and studied in detail.

## 1.1 Scope and Organization of this Work

Sunspots are one of the most prominent solar features. Under certain conditions, these dark dots on the solar disk can be seen with the naked eye. Even though records of sunspots have existed since two millennia (Wittmann and Xu, 1987), it was not until the 16<sup>th</sup> century that they were investigated systematically. While some astronomers considered them as solar features, others believed that they are caused by exosolar phenomena. An important observation was made by Hale (1908), who discovered strong magnetic fields within sunspots and proposed that these fields are caused by strong currents due to a cyclonic motion of plasma around the spot. In contrast to this idea, Evershed (1909) found spectroscopic evidence for a radial outflow of plasma in the penumbrae of sunspots.

The aim of this work is to study the small-scale structure of this so-called Evershed effect and to compare the results with predictions of penumbral models by using data of high spectral and spatial resolution obtained by HINODE.

Chapter 2 provides a brief introduction to the Sun, while the current knowledge of sunspots is summarized in Chapter 3. Chapters 4 and 5 elaborate on the method used in this study from a theoretical and experimental perspective. Chapters 6 and 7 describe the investigation of the horizontal and the vertical components of the Evershed effect, while Chapters 8 and 9 study the gradients with height of the penumbral magnetic and velocity field. In conclusion, Chapter 10 evaluates the quality of penumbral models in the light of HINODE observations.

A short summary of the contents is provided in the beginning of each Chapter. For convenience, hyperlinks are used throughout the electronic version of this text, e.g. for sections, figures, tables and references. Additionally, references may be accessed directly using the corresponding URL in the bibliography.

# The Structure of the Sun

The structure of the Sun is the result of a balance of forces (mainly between gravity and pressure), the energy balance between its generation in the core and its loss at the solar surface as well as the stationary energy transport in-between. Section 2.1 reviews the inner body of the Sun, while the atmospheric layers, including a range of observable features, are summarized in Section 2.2.

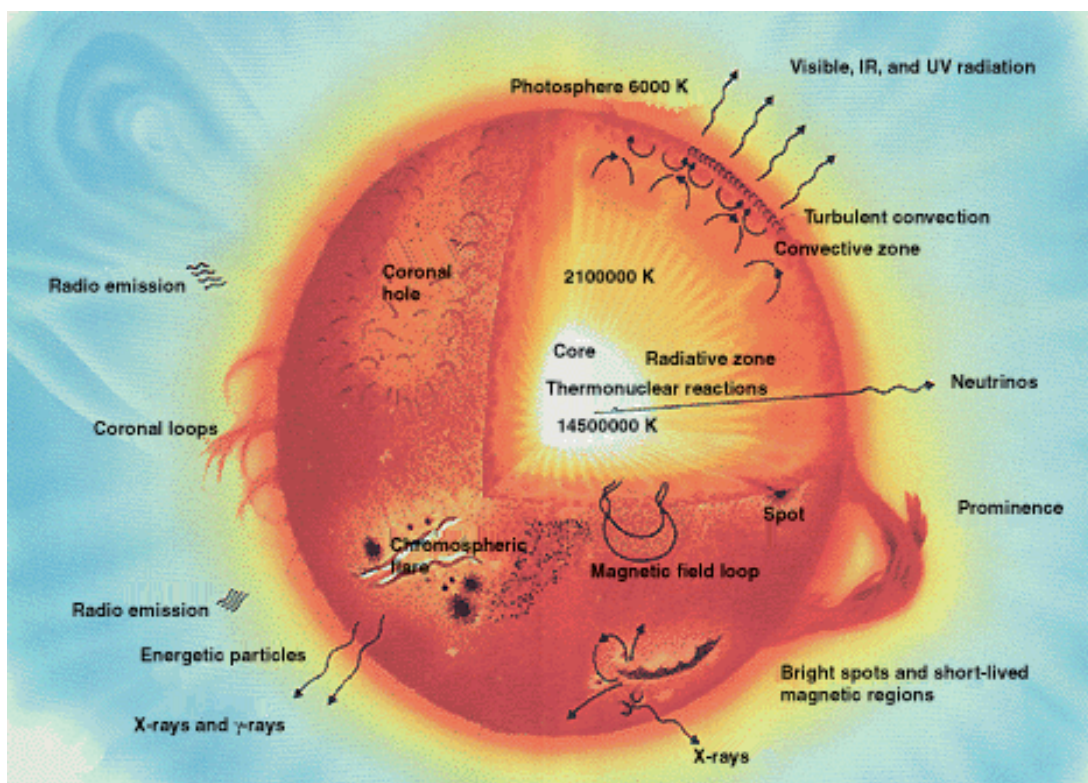


Fig. 2.1: Sketch of the structure of the Sun. Adopted from Wikipedia (2011b).

## 2.1 The Solar Interior

The solar model governing its internal structure has to obey physical laws such as the conservation of mass and momentum, and it has to describe the balance and

transport of energy. Theoretical considerations yield four first order differential and four constitutive equations. To solve the differential equations, certain boundary conditions are assumed and then modified in an iterative process until they provide reasonable observable values (Stix, 2004). The solution to these equations yields, for example, the distribution of temperature ( $T$ ), pressure and density ( $\rho$ ) with solar radius (Christensen-Dalsgaard et al., 1996).

**The Core:** In the solar core H is converted into He by nuclear fusion. This process is described by the CNO-tricycle (von Weizsäcker, 1938; Bethe, 1939) or by different proton-proton chains (Bethe and Critchfield, 1938). Measurements of the neutrino spectrum show that the latter process, which converts 7‰ of the mass of the participating particles into energy, is dominant in the Sun. The fusion rate is in an equilibrium: On the one hand, a higher rate would increase  $T$  and cause an expansion of the core, which would decrease  $T$  again. On the other hand, a lower fusion rate would cause the core to cool and shrink, increasing the fusion rate and reverting it to its current level.

**Source of Energy:** The source of the solar energy supply has long been the issue of debate. One theory proposed gravitational contraction: The Sun is collapsing slowly, thereby converting gravitational potential energy into heat and light. Taking the current solar luminosity into account, the so-called Kelvin-Helmholtz (KH) timescale would be around  $3 \cdot 10^7$  years, which was considered a good estimate of the age of the Sun in the 19<sup>th</sup> century. In the 20<sup>th</sup> century, however, geological evidence yielded an age of the Earth of the order of  $4 \cdot 10^9$  years. The resulting conflict between the geological timescale and the KH timescale was not settled until it was accepted that nuclear fusion provides another source of energy within stars. If it is assumed that 1‰ of the mass of the Sun is converted into radiant energy, the nuclear time scale is of the order of  $10^{10}$  years, i.e. the present age of the universe.

**Radiation Zone:** H and He are fully ionized within the radiation zone. Free-free absorption, bremsstrahlung and electron scattering cause the mean free path of photons of a few millimeters. With increasing radius, the gradient in  $T$  and  $\rho$  yields a cooler and thinner, hence less opaque, solar plasma. On average, the photons thus diffuse towards the outer layers, transporting the energy by thermal radiation. Estimates of the photon travel time range between  $1.7 \cdot 10^5$  years, if a random walk is assumed (Mitalas and Sills, 1992), to  $1.7 \cdot 10^7$  years, if thermal adjustment of the Sun is taken as a measure (Stix, 2003).

**Convection Zone:** Within the convection zone,  $T$  drops rapidly and allows the formation of neutral H and He. The reconnection consumes a large fraction of the free electrons, increasing the opacity until the gradient of  $T$  becomes larger than the adiabatic gradient. This triggers convective instabilities, and energy is transported by moving plasma that reaches the surface within months (Stix, 2004).

## 2.2 The Atmospheric Layers

The surface of the Sun is commonly defined as the atmospheric layer at which the solar plasma changes from opaque to transparent, or more precise, where the opacity of the solar plasma at 500 nm ( $\tau_{500}$ ) corresponds to unity. This transition depends on the wavelength (solar absorption lines) and the position on the solar disk (limb darkening effect). The fact that  $\tau = 1$  occurs at different geometrical height within an absorption line provides an important tool to study the thermodynamic state<sup>1</sup> of different atmospheric layers. Theoretical models, which have to obey observational constraints, yield a distribution of T within the atmosphere (Vernazza et al., 1981). It is remarkable that T decreases to 4100 K at a height of 500 km above  $\tau_{500} = 1$ , but then increases again, reaching several  $10^6$  K in the corona.

**Photosphere:** Convective plumes transport the hot plasma from below into the photosphere, where it cools radiatively. The top of these plumes are seen as bright elements, so-called granules. Like Bénard cells, the granules resemble a honeycomb structure of hexagonal prisms. They have a diameter of around 1000 km and a lifetime of approximately 10 minutes. However, in observations with a high spatial resolution, the granules show a substructure (Steiner et al., 2010). Between the granules, where the cooler plasma sinks back below the surface, multiply connected intergranular lanes appear. This granular pattern is called the quiet Sun (QS).

Supergranules are the giant version of granules with diameters of  $2 \cdot 10^4$  km across and are best seen in synoptic Doppler maps of the solar disk. Individual supergranules last for one or two days and have flow speeds of about  $0.5 \text{ km s}^{-1}$ .

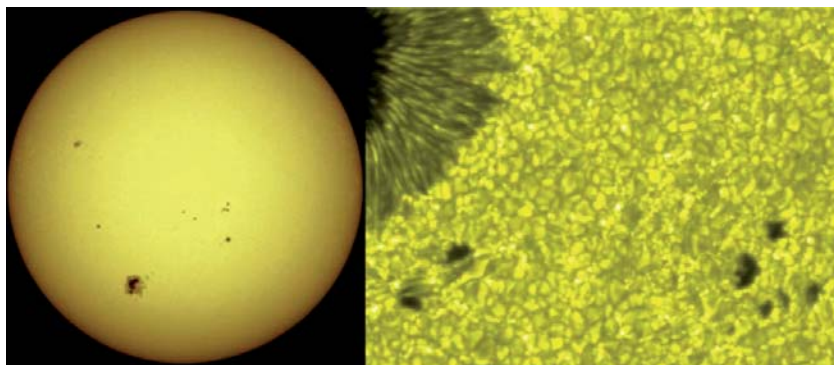


Fig. 2.2: Left: White light picture of the solar disk. Adopted from Hathaway (2007a). Right: HINODE high resolution image at 555.1 nm. Adopted from Bridgman (2007)

The QS appears darker at the solar limb when compared to the center of the disk. This is because the line of sight (LOS) penetrates the photosphere under an

---

<sup>1</sup>In the local thermodynamic equilibrium, collisions within the plasma distribute the energy equally among the degrees of freedom of the constituent particles. Thus temperature may be defined as a thermodynamic quantity. If the density decreases, collisions occur less frequently and the temperature becomes a kinetic quantity that may assume separate values for different directions or different particle species, e.g. ions and electrons. It is necessary to keep this in mind when comparing photospheric with chromospheric or coronal temperatures.

angle which is largest at the solar limb. Thus, the path through the atmosphere is increased both in length and opacity, causing the limb to appear darker since the photons stem from higher and cooler photospheric regions.

Magnetic flux concentrations alter the granular pattern, and form intergranular bright points, faculae or pores. If the pore is at least partially surrounded by a filamentary and less dark ring, it is called a sunspot<sup>2</sup> (Bray and Loughhead, 1964).

**Chromosphere:** During the totality of a solar eclipse, the chromosphere appears as a deep red ring (emission of  $H_\alpha$  at 656.2 nm) around the lunar disk. The chromosphere is the coolest layer of the solar atmosphere. Its magnetic field forms hammock-like structures, suspending plasma above the surface. Depending on whether these thread-like strands are seen on the disk or at the limb, they are called filaments or prominences respectively. Other features, i.e. plage, are often seen around sunspots. The web-like pattern at the edges of supergranular cells is called the chromospheric network and the highly dynamic magnetic fields filled with luminous gas moving up and down within 10 minutes are referred to as Spicules.

**Corona:** The outermost layer of the atmosphere, i.e. the corona, is so hot that not only H and He, but also C, Ni and O are completely ionized. Heavier trace elements, i.e. Fe and Ca, are highly ionized and cause the emission line corona. Prominent explanations for the coronal T, which seem at odds with the second law of thermodynamics, involve reconnection of magnetic field lines as well as magneto-acoustic and Alfvén waves. Coronal feature, mainly caused by the magnetic field, are: Coronal loops, solar flares, helmet streamers, polar plumes or coronal holes.



Fig. 2.3: Left: White light corona during the totality of a solar eclipse. Adopted from Hathaway (2007d). Center: Image taken in Fe IX/X at 17.1 nm which corresponds to a temperature of  $1 \cdot 10^6$  K. Adopted from TRACE (2002). Right: White light image of the SOHO coronagraph. The occulted disk is filled with an image taken by SOHO in He II at 30.4 nm, which corresponds to a temperature<sup>3</sup> of  $7 \cdot 10^4$  K. Adopted from SOHO (2007).

<sup>2</sup>This definition has been criticized by McIntosh (1981), but will be used throughout this work.

<sup>3</sup>Usually it is the collision with the electrons from the local environment that excite or ionize atoms and cause solar spectral lines. In the case of He II, non-local electrons from the hotter coronal regions cause this ionization. The temperature is inferred from model calculations similar to the VAL-C model and does not refer to the kinetic energy of the electrons, e.g. in Fe XII.

# 3

## Sunspots

Section 3.1 provides a summary of the properties of sunspots during the solar cycle as well as wide-spread ideas for the generation of magnetic fields. Part of it is based on the work of van Driel-Gesztely (2009) and van Driel-Gesztelyi and Culhane (2009). The following two Sections (3.2 and 3.3) draw a more detailed picture on sunspots, following the extensive review by Solanki (2003). The focus lies on small-scale features and their dynamical behavior in as well as around the umbra and the penumbra. Section 3.4 summarizes the current knowledge about the formation and decay of sunspots. This chapter is concluded in Section 3.5 with a discussion of different physical mechanisms explaining the Evershed flow as well as a review of the state of the art of penumbral models, including their limitations and shortcomings.

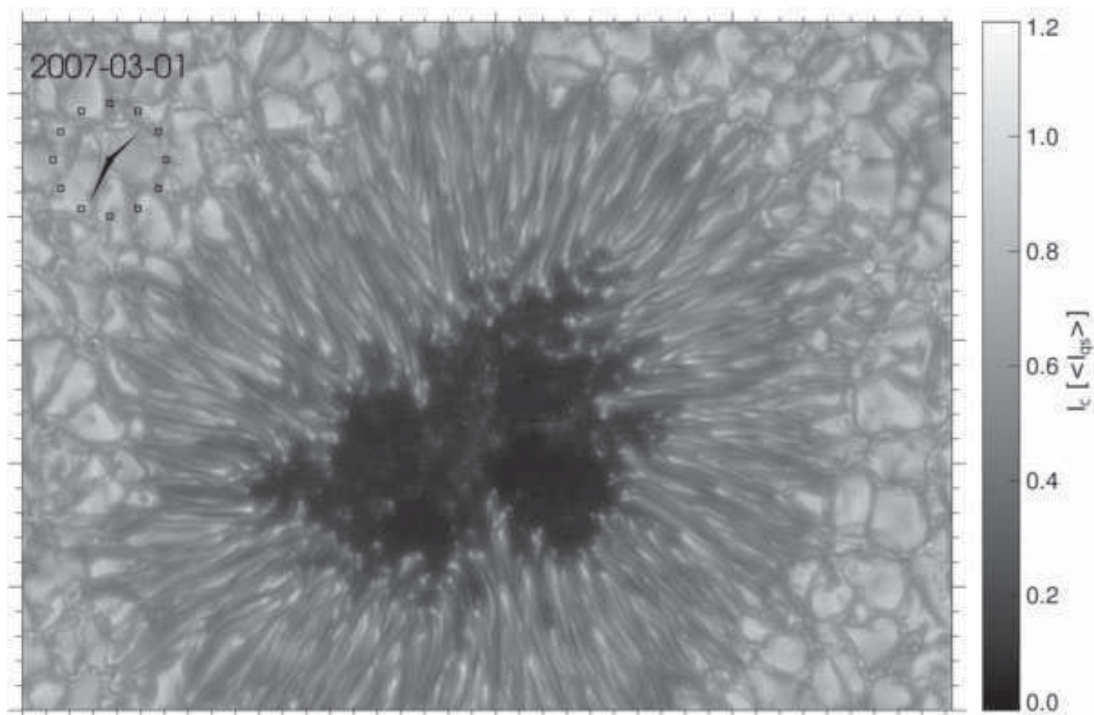


Fig. 3.1: HINODE BFI image of a sunspot taken in the blue continuum at 450.5 nm with a spatial resolution of  $0.''2$ . The image has been post-processed to increase the contrast and make the small-scale features more apparent. Tick-marks are in seconds of arc.

### 3.1 Global Properties and Periodicity

The invention of the telescope in the early 17<sup>th</sup> century led to a systematic investigation of the Sun. Daily observation of sunspots and other solar features showed that the equatorial plane of the Sun rotates roughly 20% faster than the polar regions (Scheiner, 1630; Spoerer, 1861). A closed expression for this differential rotation was first given by Carrington (1863). Modern observation of magnetic features yield  $\omega(l) = 14.38 - 1.95 \sin^2(l) - 2.17 \sin^4(l)$  for the rotational speed of the solar latitudes (1).

**Sunspot cycle:** Schwabe (1844) was among the first to report on a 11 year cycle of the apparent number of sunspots. This cycle was confirmed by Wolf (1850), who counted sunspots together with active regions. The waxing and waning of this so-called Wolf number is visible in the top panel of Fig. 3.2. Cycles with a large number of spots (during the last 50 years) and almost no spots at all (during the Maunder minimum) have been measured. To what extent this variation of solar activity might influence the terrestrial climate, i.e. result in ice ages or cause global warming, is still under debate (Jungclaus et al., 2010).

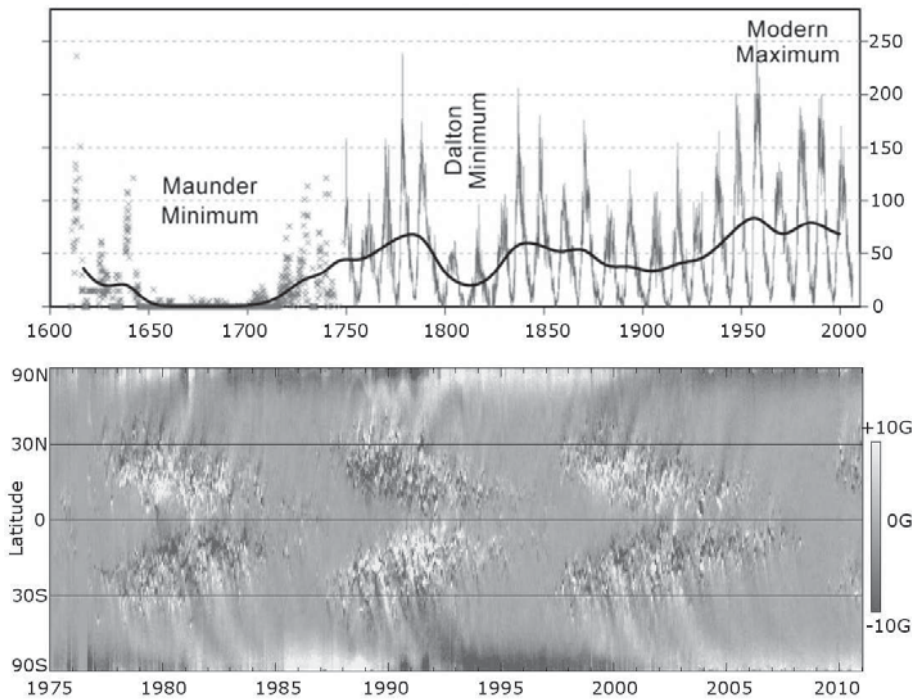


Fig. 3.2: Top: Number of apparent sunspots on the Sun – before 1750 only sporadic observations. Adopted from Wikipedia (2011a). Bottom: Modern butterfly diagram of the last three solar cycles. Adopted from Hathaway (2007b).

Carrington (1858) noted that sunspots appear at progressively lower latitudes as the solar cycle evolves. This was confirmed by Spoerer (1883), who visualized this effect by calculating the solar area occupied by spots in a certain time interval and plotted this versus the solar latitude. The result can be seen in the lower panel

of Fig. 3.2. The spots appear around  $30^\circ$  north and south of the equator in the beginning and emerge close to the equator at the end of the sunspot cycle. The region between  $\pm 30^\circ$  latitude is called the activity belt because sunspots usually do not appear at larger latitudes. Since the distinct pattern in the activity belt resembles the shape of the wings of a butterfly, Spörer's plot is often referred to as the butterfly diagram<sup>1</sup>. The Wolf number reaches its maximum in the middle of the cycle when the majority of sunspots appear at  $\pm 15^\circ$  latitude.

After the discovery of solar magnetic fields by Hale (1908), it was recognized that sunspots are only the most prominent manifestations of solar magnetism and can be used as a proxy of the latter. Since areas of increased magnetic activity – i.e. active regions (ARs) – typically have a bipolar structure and sunspots are always located within such regions, they often appear in binary groups. The western or preceding (p) spot of such a group is usually larger and the first to be formed, while the eastern or following (f) spot appears later, frequently splits into several components and disappears sooner.

**Hale's law:** Hale and Nicholson (1925) not only reported that the polarity of the magnetic field is opposite in p- and f-spots, but also found that the magnetic field in binary ARs is of opposite polarity in both hemispheres as well as in subsequent sunspot cycles. This behavior, which is called Hale's law, is shown in the left panel of Fig. 3.3. During the 14<sup>th</sup> cycle, the polarity of p-spots was negative in the northern hemisphere, while the respective spot in the southern hemisphere showed positive polarity. In the 15<sup>th</sup> cycle, this pattern was just the opposite.

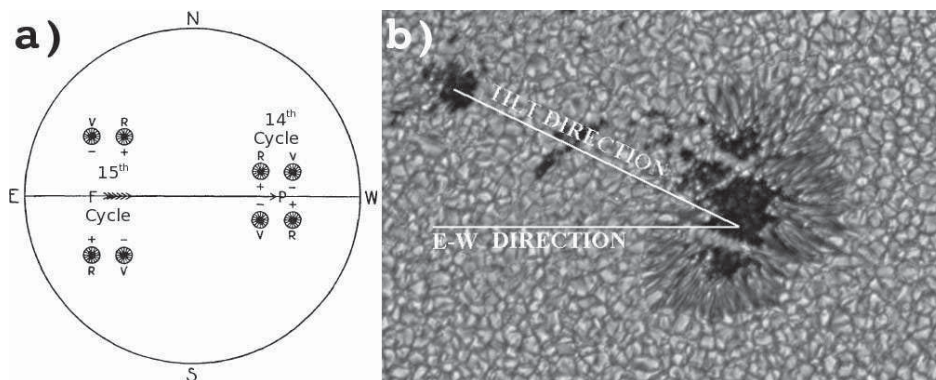


Fig. 3.3: Left: Hales law states that the polarity of the p- and f-spots is opposite in different hemispheres and opposite within one hemisphere and different cycles. Adopted from Hale et al. (1919). Right: The tilt angle between the axis of a bipolar AR and the equator is described by Joy's law. Adopted from Hathaway (2007b).

Hale's law does not only apply to sunspots and AR, but also to the polarity of the average magnetic field in the respective hemispheres. This phenomenon is depicted in the lower panel of Fig. 3.2. During the maximum of the 22<sup>nd</sup> cycle,

<sup>1</sup>In addition to the original butterfly diagram, the lower panel of Fig. 3.2 shows the polarity of the magnetic fields. Spörer was not able to measure solar magnetic fields, but only the sunspot area as a function of latitude.

( $\approx 1980$ ), the northern hemisphere showed more positive polarity, while the southern hemisphere was dominated by negative polarity. During the maximum of the 23<sup>rd</sup> cycle ( $\approx 1991$ ), this configuration was reversed, while in the 24<sup>th</sup> cycle ( $\approx 2002$ ), it was the same as in the 22<sup>nd</sup>. In conclusion, the period of a solar cycle – i.e. the time until the magnetic field in one hemisphere shows the same polarity again – actually amounts to 22 years<sup>2</sup> (Hale and Nicholson, 1938).

Bipolar regions that obey Hale’s law are referred to as Hale oriented. Anti-Hale orientated AR occur preferentially in the end of a sunspot cycle, when magnetic flux with the configuration from the previous cycle emerges close to the equator, while flux emerging in higher latitudes already belongs to the present cycle.

**Joy’s law:** Careful analysis of a large number of bipolar sunspots led to the conclusion that, throughout the cycle, f-spots appears at higher latitudes when compared to the position of the p-spots – cf. right panel in Fig 3.3 and Hale et al. (1919). This behavior, as well as the fact that the tilt angle between the axis of the bipole and the equator becomes larger for increasing latitude, is called Joy’s law. More recent studies indicate that it is rather the distance between the spots within the bipolar ARs which is correlated with the tilt angle (Fisher et al., 1995).

**The Babcock Model:** A conceptual model explaining the evolution of the magnetic field during the 22-year solar cycle was put forward by Babcock (1961).

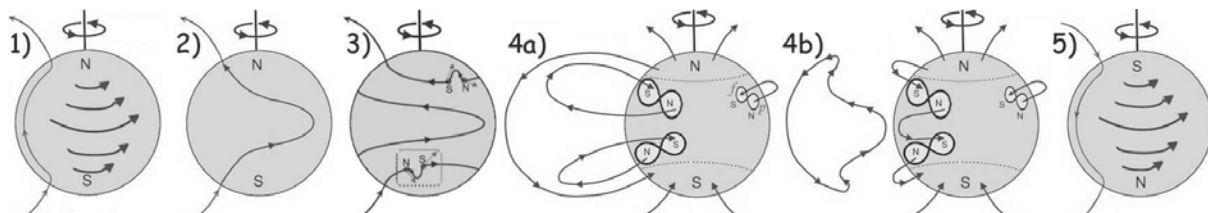


Fig. 3.4: Magnetic field configuration during the solar cycle according to Babcock (1961).

1) The magnetic field is an axisymmetric dipole, in which the lines of force lie in meridional planes and loop out from the north pole (positive polarity). They cross the equatorial plane at some distance and re-enter the Sun at the south pole (negative polarity). Only latitudes larger than  $\pm 55^\circ$  show magnetic activity.

2) As the magnetic field lines are frozen<sup>3</sup> into the solar plasma, the differential rotation of the Sun shears the poloidal field into a toroidal configuration (Bullard and Gellman, 1954), thereby amplifying its initial strength thousandfold.

<sup>2</sup>The polarity of magnetic features at the poles does not change simultaneously with the polarity of sunspots in the activity belts, but approximately at the maximum of the sunspot cycle.

<sup>3</sup>A combination of the laws by Ohm, Ampère and Gauß yields the induction equation, containing a conductive and a diffusive term. Since the conductivity of the solar plasma is orders of magnitude higher than its diffusivity, the latter can be neglected. In other words, the time scale for the magnetic field to diffuse through the solar plasma is so large that the field lines appear to be attached to (or frozen into) the plasma itself.

3) This amplification is maximal around  $l = \pm 30^\circ$ . If flux tubes with Kilogauss field strength are obtained, they become buoyant and start to rise in the form of an  $\Omega$ -loop (Parker, 1955b). When they erupt through the surface, they form a bipolar AR with opposite magnetic polarities, reversing their orientation across the equator. The drift of AR towards the equator during the sunspot cycle is a consequence of the differential rotation of the Sun.

4) The reversal of the poloidal field is due to the systematic inclination of ARs. The p-polarity moves towards the equator, where it neutralizes with the opposite polarity from the other hemisphere, while the f-polarity drifts towards the nearest pole, where it eventually reverses the polarity of the polar field<sup>4</sup>.

5) A poloidal field configuration of reversed polarity is obtained after 11 years. Analogues to steps 2), 3) and 4) complete the whole 22-year magnetic cycle.

### Generation of Magnetic Fields:

It is assumed that solar magnetic fields are generated by a dynamo process operating in the tachocline<sup>5</sup>. Elaborated dynamo models try to combine the induction equation with the coupled mass, momentum and energy relations for the plasma, to obtain a dynamo equation. However, since the tachocline cannot be measured directly by existing helioseismologic techniques (van Driel-Gesztelyi and Culhane, 2009), all models must rely both on theoretical considerations and on boundary conditions inferred from observations.

Common to all dynamo models are the so-called  $\alpha$ - and  $\omega$ -effects. The  $\omega$ -effect describes the shear of an initial poloidal field into a toroidal configuration, as well as its resulting amplification, by the differential rotation of the Sun. The reversed transformation, from the toroidal back into a poloidal configuration, is more difficult to describe. Parker (1955a) showed that the plasma within the convection zone is subject to Coriolis forces which induce helicity in such a way that the zonal magnetic field gains a meridional component. As a result of this  $\alpha$ -effect, rising magnetic elements carry a poloidal field component opposite to the present cycle (Parker, 1970).

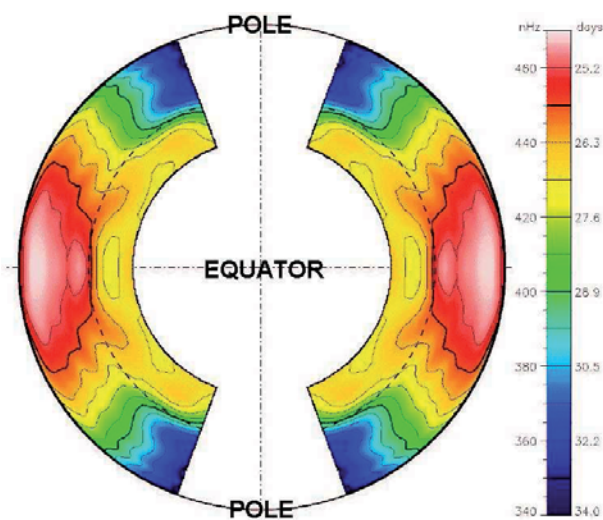


Fig. 3.5: Differential rotation in the solar convection zone. The equator rotates faster than the poles. Adopted from (Hathaway, 2007c).

<sup>4</sup>Leighton (1969) interpreted the mean flux transport as the combined effect of the dispersal of magnetic elements by a random walk process and the asymmetry in the flux emergence as stated by Joy's law. He included the flux transport in a quantitative, closed kinematic model for the solar cycle called the Babcock-Leighton model.

<sup>5</sup>The tachocline is a thin shell at the base of the solar convection zone, where the latitudinal differential rotation interferes with the solid rotation of the solar radiative core (Gilman, 2005).

Even though the details of the dynamo process are still under debate, substantial progress has been made by modifying the dynamo equations to account for the meridional circulation. This flow influences the configuration of the global magnetic fields during a solar cycle (Choudhuri et al., 1995; Dikpati and Charbonneau, 1999), and calculations with an advective dynamo model have shown that it aids the transformation of the toroidal field back into a poloidal configuration with opposite polarity at the end of the solar cycle (Dikpati and Gilman, 2001a,b)

## 3.2 The Umbra

In the umbra, convective motions are suppressed by the strong magnetic field, and radiative losses cannot be balanced by energy from the solar interior. Thus, the umbra is cooler than the surrounding QS and appears dark in continuum observations. The umbral brightness is not uniform, but exhibits cellular variations of intensity. The dark nuclei (DN) cover about 10% to 20% of the umbral area and have a size and temperature of approximately  $1.''5$  and 3500 K. They are the darkest part of the umbra and show, depending on wavelength, only 5% to 30% of the continuum intensity of the QS (Sobotka et al., 1991). In contrast to the diffuse background, DN show almost no variation in brightness (Livingston, 1991).

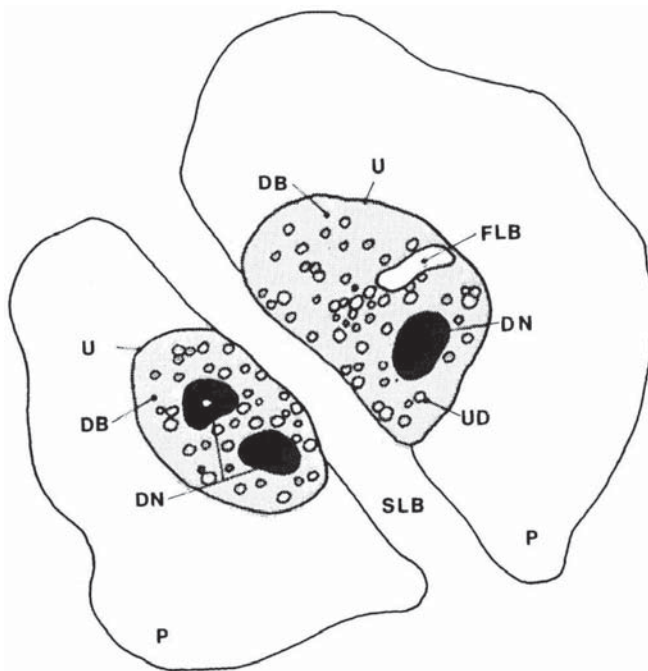


Fig. 3.6: Schematic drawing of umbral features. P: penumbra, U: umbra, SLB: strong light bridge, FLB: faint light bridge, UD: umbral dot, DB: diffuse background, DN: dark nucleus. Adopted from Sobotka et al. (1993).

**Umbral Dots:** Small and bright intrusions, called umbral dots (UDs), cover 3% to 10% of the umbral area, but contribute 10% to 20% to its brightness (Sobotka et al., 1993). Usually, a distinction is made between peripheral umbral dots (PUDs), which move from the outer umbra to its center, and central umbral dots (CUDs), which remain fixed and are slightly darker than PUD (Grossmann-Doerth et al., 1986). There is evidence that UD are elevated with respect to the umbral background and that they are about 700 K to 1000 K hotter than the DN (Sütterlin and Wiehr, 1998; Tritschler and Schmidt, 2002). Reports of the lifetime and size of UD range from 3 to 80 minutes (Kusoffsky and Lundstedt, 1986; Ewell, 1992; Riethmüller et al., 2008) and from  $0.''1$  to  $0.''8$  respectively (Koutchmy and Adjabshirzadeh, 1981; Rimmele, 1997; Sobotka and Puschmann, 2009).

It is assumed that umbral dots are due to convection in field free gaps below the surface (Parker, 1979). This idea is supported by the simulation of Schüssler and Vögler (2006) in which UD's are caused by an altered mode of magnetoconvection in regions of weak magnetic field below the umbra. The hot plasma in these regions provides an energy reservoir for convective motions, which not only cause the bright UD's at the surface, but also decrease the field strength within them. The predicted Doppler velocity pattern in and around UD's was confirmed in observation (Ortiz et al., 2010). Additionally, the upflow within UD's shifts the  $\tau = 1$  level into cooler atmospheric regions. This explains the dark lane across the UD, which is visible in observation with a resolution better than  $0.''2$  (Bharti et al., 2007; Sobotka and Puschmann, 2009).

**Light Bridges:** Long bright structures crossing the dark umbrae of sunspots are called light bridges (LBs). They are classified according to their fine structure and brightness. Sobotka (1997) distinguishes between: Granular LBs, which harbor cells that are similar but smaller than granulation cells in the QS, and filamentary LBs, which look like intrusions of penumbral filaments. Both types of LBs may appear either as a strong or a faint feature, separating the umbra or being part of it. Strong granular LBs usually evolve into regions of regular granulation splitting the spot, while faint filamentary LBs seem to be associated with PUDs. It is an established fact that LBs harbor convective flows and contain a weaker (reduction of 1.5 kG) and more inclined (zenith angle of  $5^\circ$  to  $30^\circ$ ) magnetic field (Rimmele, 1997, 2008; Berger and Berdyugina, 2003; Jurčák et al., 2006). With sufficient spatial resolution, a dark lane is visible along the main axis of the LB. It is approximately  $0.''5$  wide, produces small barb-like extensions to the sides and is elevated above the umbral background (Berger and Berdyugina, 2003; Lites et al., 2004).

**Wilson Depression:** Wilson and Maskelyne (1774) first noted that the limbward penumbra appears broader when compared to its center-side part, if a sunspot is observed at the edge of the solar disk. This phenomenon is interpreted as a geometrical effect. Due to the depression of the umbra, the sunspot forms a dip resembling the shape of a funnel in the solar surface.

Today it is accepted that the magnetic field causes this depression, because lateral pressure balance requires that the gas pressure, hence density and opacity, in the umbra is lower when compared to the QS. Furthermore, the cool umbral atmosphere is per se more transparent, since the  $H^-$  bound-free opacity – the major contribution to photospheric opacity – is very sensitive to temperature. Thus, depending on the size of the spot, the umbral surface ( $\tau_{500} = 1$ ) is located 500 to 800 km below<sup>6</sup> that of the QS (Bray and Loughhead, 1964; Stix, 2004).

---

<sup>6</sup>In the penumbra, the complex filamentary structure makes it difficult to convert a  $\tau$  scale, e.g. from inversion results, into a geometrical height scale. This is because strong jumps of the  $\tau_{500} = 1$  surface occur within distances of less than  $1''$  (Puschmann et al., 2010).